International Journal of Multiphysics
Volume 18, No. 4, 2024
ISSN: 1750-9548

Optimizing the Aerodynamics of Bluff Bodies Applying the Adjoint Method

Behrooz Shahriari[1], Hamid Farrokhfal[1*], Mohammad Reza Nazari[2]

[1]Associate Professor, Faculty of Mechanics, Malek Ashtar University of Technology, Isfahan, Iran

[2]PhD Student, Faculty of Mechanics, Malek Ashtar University of Technology, Isfahan, Iran

*Corresponding author

Abstract

Nowadays, afterburner is considered a fundamental component of aircraft turbine engines, which results in increased engine thrust. Flame stability is an essential condition for proper functioning of the afterburner. Given that the afterburner activation leads to increased fuel consumption and a rise in aircraft temperature, its usage is limited to brief and specific periods such as during aircraft takeoff, specialized maneuvers, and instances requiring maximum aircraft speed. The engine's performance can be divided into two modes: with afterburner on and off. The presence of bluff bodies ensures flame stability in afterburner-on mode, whereas in afterburner-off mode, bluff bodies contribute to increased pressure loss. Optimizing the geometry of bluff bodies can reduce drag and consequently decrease pressure loss in afterburner-off mode. The adjoint method based on gradient optimization method has garnered increased focus due to its remarkable efficiency in determining the sensitivity of objective with respect to geometric parameters. In this study, the geometry of a bluff body in afterburner unit of a turbine engine is optimized to reduce drag. Initially, to validate the simulation, the bluff body is simulated in both afterburner-on and off modes, ensuring the reliability of simulation method. Subsequently, bluff body's geometry is optimized to reduce drag. produced drag by flame holder and recirculation zones behind it are evaluated as two important factors in assessing the performance of flame holder in both reacting and non-reacting modes. The results indicate that in the optimized geometry, drag is reduced by 27%, and combustion efficiency is increased by nearly 3%.

Keywords: Turbine engines, Bluff body, Drag, Adjoint method, Numerical simulation, Flame holder.

1-Introduction

One of the methods to increase the thrust of turbojet engines without increasing the volume and weight of the engine is the use of afterburners. Flame stability in ramjet engines and afterburners used in turbojet and turbofan engines is typically achieved through the use of a bluff body [1]. The bluff body contributes to flame stability in combustion systems by creating a recirculation zone downstream [2].

During afterburner-off conditions, the bluff body causes an increase in pressure loss [3]. Therefore, in these conditions, the aerodynamic shape of the bluff body significantly influences the level of pressure loss. One of the methods to reduce drag and pressure loss is to decrease the width of the flame holder [4]. Mohamed et al. effectively reduced drag by modifying the corners of the bluff body through reducing the wake width [5]. However, changing the width of the flame holder affects flame formation and stability [6]. Herbert studied how wake aerodynamics and drag coefficient affect the stability boundaries of flames [7]. In the afterburner-on mode, pressure loss is necessary to stabilize flame and combustion [8]. However, achieving complete combustion is not feasible under low-pressure conditions. Therefore, striking a balance between these two factors is highly important [9]. Another method for reducing drag involves altering the arrangement of flame holders. The arrangement of

flame holders should be such that, in addition to facilitating stable combustion, it mitigates flow blockage effects, which lead to pressure loss [10-11]. In addition to the above considerations, the V-gutter apex angle also influences flow behavior. Yong et al. demonstrated that increasing the interior apex angle of V-gutter flame holder results in a larger recirculation zone, leading to an increase in backflow velocity and ultimately widening of the flame [12]. Furthermore, increasing the apex angle of the V-gutter bluff body extends flame stability [13, 14].

In the past decade, various optimization approaches have been employed for different purposes in the design of flame holders. K. Karthik and colleagues optimized a bluff body in the form of a circulate cylinder to reduce drag and noise using CFD. They utilized a multi-objective algorithm based on the swarm optimization method [15]. Li et al. optimized the combustion efficiency of a scramjet engine in an intelligent strut design under different operating conditions. The results indicated an increase in combustion efficiency by up to 8.22% and a reduction in force by 66.12% in the new configuration [16]. Povinelli et al. conducted simulations on struts, exploring six structural factors including the radius of the leading edge, maximum thickness position, thickness ratio, sweep angle, and strut length. The results indicated that the thickness ratio is the primary factor contributing to drag reduction [17]. Tao Cai focused on numerically optimizing the location of the bluff body and the configuration of the combustion chamber. Their work resulted in a notable improvement in combustion efficiency compared to the baseline case, although pressure loss also increased [18]. Additionally, Tomas Oberg applied Design of Experiments (DOE) to optimize carbon monoxide in an industrial afterburner [19]. Among the optimization methods used in aerodynamic problems, the adjoint method has garnered more attention due to its capability to efficiently compute the derivatives of objective functions for multiple design variables [20, 21]. J. Brezillon employed the adjoint method to reduce drag under conditions of constant lift and pitching moment on an airfoil [22]. Juanmian Lei developed a framework to design the aerodynamic shapes and optimize airfoils with low Reynolds numbers using laminar unsteady equations and the adjoint method [23]. The adjoint method is also well-suited for optimization in complex geometries. Md Araful Hoque optimized the nose of a car, resulting in a 27% reduction in drag and fuel consumption [24]. Harry Day optimized the shape of a blade and demonstrated that the adjoint method is an efficient approach for aerodynamic problems [22].

In the current study, numerical simulations were conducted for both combusting and non-combusting conditions on a bluff body. Subsequently, using the adjoint method, the geometry of the bluff body was optimized to reduce drag. With this approach, after the initial solution of flow, sensitive geometric points are identified, and optimization moves towards improving the objective of the problem. In the optimized design, in addition to drag reduction, combustion efficiency has also increased.

2- Objective Function and Adjoint Optimization Process:

The objective of optimizing a system is to minimize or maximize a function, which serves as a measure of the system's performance. In aerodynamic designs, this function can take various forms, such as lift coefficient, drag coefficient, or lift-to-drag ratio. In the present study, the objective function is the drag coefficient, a dimensionless quantity that relies on the geometric body shape and defined as follows:

$$C_D = \frac{2F_D}{A\rho u_\infty^2} \qquad (1)$$

Where, A, ρ, u_∞, and C_D represent the projected frontal area, density, freestream velocity, and drag coefficient of the body, respectively.

The Adjoint Method is a specialized mathematical tool that can be used to compute the derivatives of engineering quantities with respect to all system inputs, including flow geometry. It is a gradient-based method where the sensitivity required in the optimization process is obtained from an equation called the adjoint equation, rather than directly calculating it [23]. In discrete adjoint method, the flow's governing partial differential equations (PDEs) are discretized first, and then differentited to establish discrete adjoint equation. In contrast, the continuous adjoint method begins by formulating adjoint equations through differentiation of the governing PDEs, which are subsequently discretized for solving. The optimization cycle involves a common process between the solver for the flow based on the Navier-Stokes equations and the adjoint solver. Figure 1 summarizes the optimization cycle. According to Figure 1, the flow equations are initially solved, and then the results are fed into the adjoint solver

to compute sensitivity information, resulting in the determination of geometry sensitivity to the objective function. Subsequently, depending on sensitivity level, adjustements are made to the body geometry. Finally, the flow field is recalculated based on the new geometry, and objective function's results is evaluated. This loop continues until the desired value of the objective function is achieved.

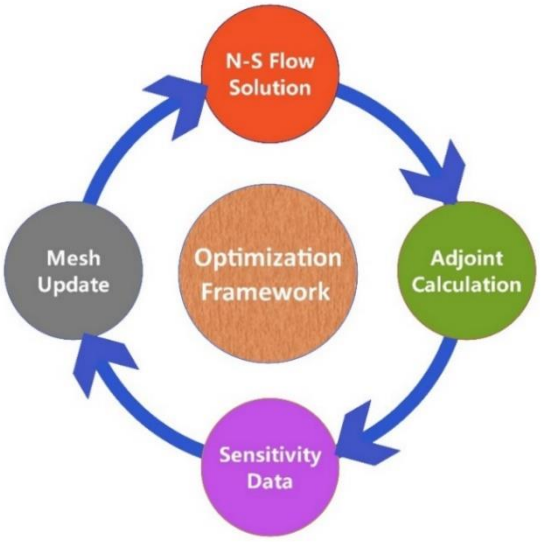

Fig 1: *Adjoint shape optimization workflow*

The adjoint objective (d) is a function of both the state of the flow $\emptyset$ and the control variables (c), such as the geometry x_i, as shown in equation (18). In the present work, the control variables consist of the points that delineate the surfaces of the bluff bodies:

$$d = d(\emptyset(c).c) \qquad (2)$$

The adjoint equations are formulated based on derivative terms derived from the initial flow solution, as stated hereunder:

$$R(\emptyset(c).c) = 0 \qquad (3)$$

In the present work, the objective function is the drag force, which is defined as an observable quantity. Therefore, the Lagrange multiplier is formulated as follows:

$$L(q.c.\lambda) = J(q.c) - \lambda^T R(q.c) \qquad (4)$$

Where λ is the adjoint parameter. Then, observable derivative in relation to the design variables is given by:

$$\frac{dJ}{dc} = \frac{dL}{dc} = \frac{\partial L}{\partial c} + \frac{\partial L}{\partial q}\frac{\partial q}{\partial c} = \frac{\partial J}{\partial c} + \frac{\partial J}{\partial c}\frac{\partial q}{\partial c} - \lambda^T\left(\frac{\partial R}{\partial c} + \frac{\partial R}{\partial q}\frac{\partial q}{\partial c}\right)$$

$$= \frac{\partial J}{\partial c} + \lambda^T\frac{\partial R}{\partial c} + \left(\frac{\partial J}{\partial q} - \lambda^T\frac{\partial R}{\partial q}\right)\frac{\partial q}{\partial c} \qquad (5)$$

Lets:

$$\left(\frac{\partial R}{\partial q}\right)^T \lambda = \left(\frac{\partial J}{\partial q}\right)^T \qquad (6)$$

Hence, the sensitivity of the observable turns out to be:

$$\frac{dj}{dc} = \frac{\partial J}{\partial c} + \lambda^T\frac{\partial R}{\partial c} \qquad (7)$$

The sensitivity equation for each mesh node in the CFD model is evaluated, and then the mesh is corrected [24]. In the present work, for shape sensitivity, the input vector c is considered as the locations (x, y) for each node in the model.

3- Validation:

To determine the accuracy and reliability of the obtained results, numerical and experimental results need to be compared. The validation study examines a premixed flame stablized by a bluff-body, conducted under the auspices of Volvo [25]. Several experimental studies [26-27] and numerical simulations [28-30] based on the Volvo work have been conducted before. Figure 2 depicts the schematic of the Volvo combustion system. This system comprises a rectangular duct with an equilateral triangular bluff body. The bluff body is in the form of an equilateral triangle, with each side length measuring to D=4cm. A premixed fuel-air mixture with a mass flow rate of 0.2083kg/s, constant temperature of 288K, and equivalence ratio of 0.65 is introduced into the channel. Propane is used as the fuel, which is mixed with air at 288K temperature.

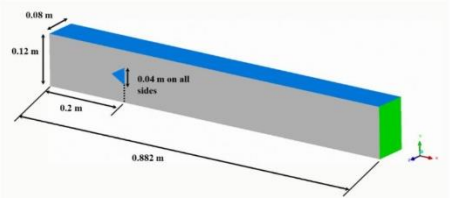

Fig 2: *Simulation set up for Volvo bluff body MVP workshop [30]*

In the present study, boundary conditions include a designated mass flow rate at the inlet and maintain a constant pressure at the outlet. The k-ω shear stress transport (SST) model was employed for modeling of turbulence, which has been validated as an appropriate choice for bluff body simulations [31-32]. The conducted simulation was two-dimensional, the domain of which is illustrated in Figure 3:

Fig 3: *CFD model geometry*

The results of the solution are investigated for both non-reactive and reactive flow conditions across numerous planes along the length of the rectangular channel. In Figure 4, the inlet velocity profile is depicted for x/D=0.375 and x/D=0.375 planes along the flame. The results indicate that the numerical solution exhibits acceptable accuracy compared to experimental data. However, there is slight deviation from the experimental results in estimating the recirculation zone length downstream of bluff-body, which could be attributed to simplifications made in the simulation. Furthermore, the findings show that the velocity is around zero in the vicinity of walls. By moving towards the centerline, the velocity initially increases and then decreases again due to the swirling and recirculating flows, and even becomes negative in some points.

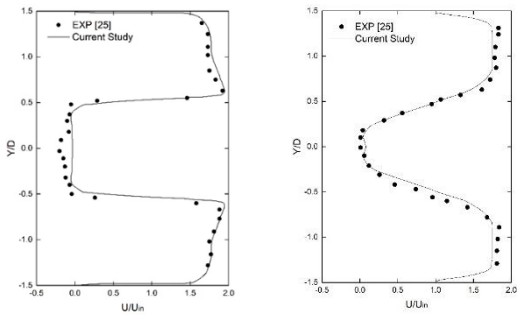

(a)=x/D=0.375 (b)=x/D=3.75

Fig 4: *The dimensionless mean inlet velocity profiles over different axial planes along the flame axis for both quantitative and experimental results*

Figure 5 illustrates the dimensionless mean temperature profiles for the axial planes at x/D=0.375 and x/D=0.375 along the flame axis for the scenario involving a reacting flow. The results indicate that after the flame formation in the zone behind the bluff body, the temperature increases. As the distance from the bluff body increases (moving from the x/D=0.375 plane to the x/D=0.375 plane), the flame expands, leading to an increase in the temperature near the walls. The quantitative results indicate a satisfactory correlation with the experimental data, indicating that the simulation has been properly conducted.

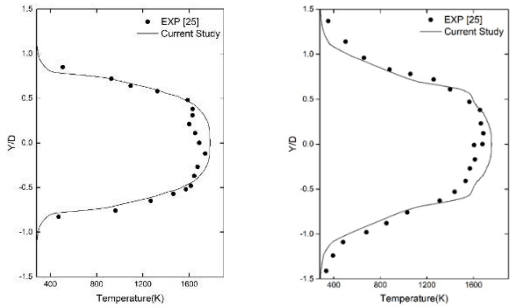

(a)=x/D=3.75 (b)=x/D=9.75

Fig 5: *The mean temperature profiles in various axial planes along the flame axis for both numerical and experimental results.*

4- Aerodynamic Optimization:

4-1 Sensitivity:

The adjoint solver calculates the sensitivity of surface by utilizing the solution of primal flow. This offers the necessary data to identify the areas that are more sensitive to geometric alteration aimed at achieving drag reduction. Figure 6 illustrates the surface sensitivity map, where regions in red indicate higher sensitivity to drag. By making relatively small geometric changes in these areas, significant alterations in drag can be achieved.

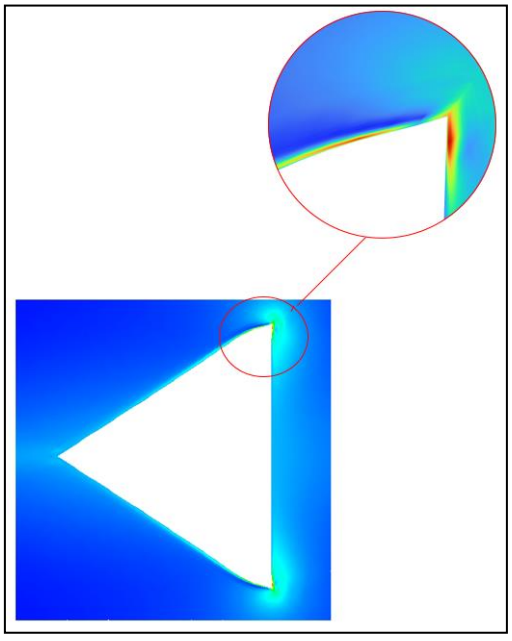

Fig 6: *Drag sensitivity on the bluff body for shape optimization*

As evident in Figure 6, the regions near the top and bottom boundaries of the bluff body exhibit the highest surface sensitivity. In Figure 7, the original and optimized geometries are illustrated, showing that as expected, the most significant alterations have occurred near the periphery of the bluff body's edge.

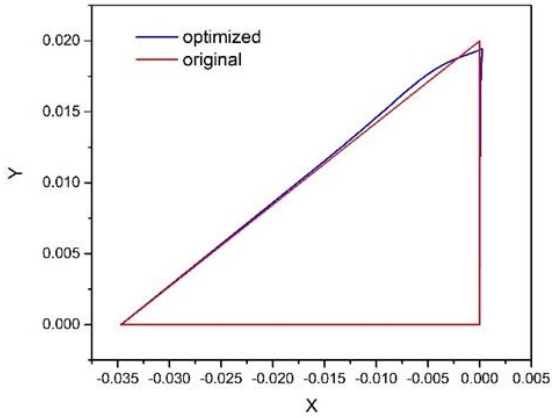

Fig 7: *Comparing the original geometry with the optimized geometry*

4-2 Optimized Results:

The optimized results include an assessment of the bluff body's performance, vortex lengths, drag, and combustion parameters for both the original and optimized geometries in both reactive and non-reactive flow conditions. The bluff body's geometric shape causes the distance between the vortices of the bluff body and duct to act as a nozzle and increase the flow velocity. Figure 8 compares the velocity contours for the optimized and original configurations. The results indicate that the overall flow pattern has not undergone significant changes, and the optimized design has managed to optimize drag with minimal alterations to the velocity field within the channel.

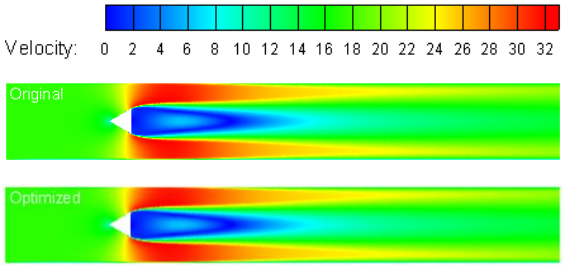

Fig 8: *The velocity contours for the original and optimized configurations under non-reacting conditions*

Figure 9 illustrates the velocity contours with streamlines in the cold flow condition. Right after the bluff body, two pairs of vortices are formed, which are linked to the flow reversing towards the hind side of the bluff body. These vortices are induced by unfavorable pressure gradient, which is dependent on the enlargement of bluff body's downstream flow region. The results indicate that after geometry optimization, the flow passing over the body exhibits better alignment, and the length of the vortex region is reduced in the optimized configuration. Consequently, the drag is reduced by 27%.

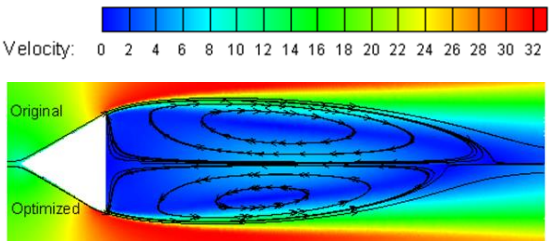

Fig 9: *The velocity contours along with streamlines for the original and optimized configurations in the non-reacting condition*

The drag reduction is accompanied by a decrease in the length of the vortices. Therefore, the length of the vortices formed in the reacting condition should also be studied. Figure 10 depicts the temperature contours in the reacting condition. The results indicate that, similar to the original configuration, in the optimized configuration, flame

vortices are formed immediately after the bluff body due to the swirling flow, creating a high-temperature region that extends to the end of the channel. Additionally, in the optimized configuration, due to better alignment of the bluff body with the flow, the width of the flame right after the bluff body is reduced compared to the original configuration. However, there is not much change observed in the flame region towards the end of the channel.

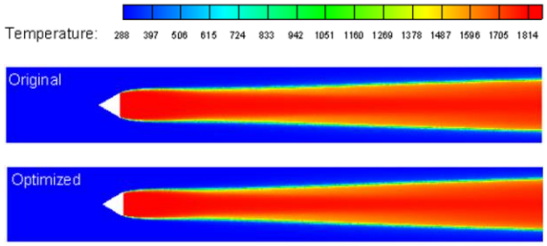

Fig 10: *The temperature contours for the original and optimized configurations*

Figure 11 depicts the temperature contours with streamlines in the reactive flow condition. Similar to the cold flow case, two vortices form just behind the bluff body, contributing to flame stability. The results indicate that in the optimized configuration, there exists a shorter vortex compared to the baseline case, which may affect flame stability.

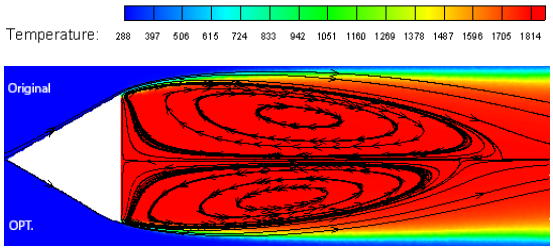

Fig 11: *The temperature contours with streamlines for the original and optimized configurations under reacting flow conditions*

Combustion efficiency is another important parameter while assessing afterburner, which is related to the geometry of the bluff body. In this study, due to the uniform distribution of the fuel-air mixture at the inlet, some of the fuel passing near the walls does not combust, resulting in low combustion efficiency. Figure 12 compares the drag and combustion efficiency for the original and optimized geometries. The results indicate that in addition to a 27% drag reduction in the optimized design, the flow passage velocity in this area decreases due to the reduction in the distance from the bluff body to the duct in the optimized geometry. This allows more time for fuel particles to undergo combustion, ultimately increasing combustion efficiency compared to the original geometry.

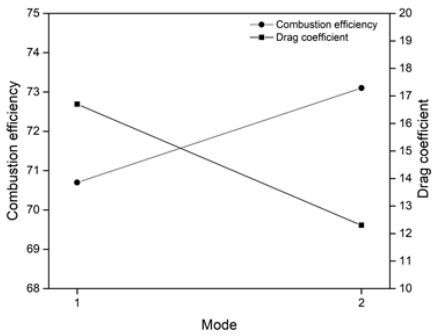

Fig 12: *The comparison of drag coefficient and combustion efficiency for the original geometry (Mode 1) and the optimized geometry (Mode 2)*

5- Conclusion:

In this study, aerodynamic optimization of a bluff body was conducted using the adjoint method. The drag and the size of recirculation zone in both reactive and non-reactive conditions were investigated, yielding the following results:

1. The results demonstrate that the adjoint optimization method, by identifying the geometry sensitiveness to the function of objective, can significantly optimize the function of objective with minimal changes to the geometry and flow pattern.

2. The reduction in the drag coefficient of bluff bodies is frequently associated with the reduction in the vortices' length, which can affect the flamestability. Therefore, studying both the length of vortices and drag coefficient simultaneously is essential for a comprehensive understanding of the problem.

3. Considering that aircrafts spend most of their flight time in afterburner-off conditions, a 27% reduction in drag can have a significant impact on reducing pressure loss and improving the aircraft performance.

4. In the optimized geometry, in addition to drag reduction, combustion efficiency has also increased. These changes result in reduced fuel consumption and potentially improved flight endurance.

Acknowledgments:

We would like to express our sincere gratitude to all those who have contributed to the successful completion of this research. We would also extend our thanks to the research team at Malek-Ashtar University of Technology for their support and collaboration.

References:

1. Bush, Scott M., and Ephraim J. Gutmark. "Reacting and nonreacting flowfields of a V-gutter stabilized flame." AIAA journal 45.3 (2007): 662-672, https://doi.org/10.2514/1.22655
2. Santosh J. S, Sajjad H, Tim L. Lean blowoff of bluff body stabilized flames Scaling and dynamics. Progress in Energy and Combustion Science 35 (2009) 98–120, https://doi.org/10.1016/j.pecs.2008.07.003
3. Malakonda Reddy Lekkala a, Mohamed Latheef a, Jae Hwan Jung b, Andrea Coraddu c, "Recent advances in understanding the flow over bluff bodies with different geometries at moderate Reynolds numbers,", Ocean Engineering 261 (2022) 111611.
4. S. Nakanishi, W. Velie, W.L. Bryant, An investigation of effects of flame-holder gutter shape on afterburner performance, Tech. Rep. Arch. Image Libr.(1954). https://ntrs.nasa.gov/citations/19930088008
5. Mohamed IK, Aissa WA. Effect of corner modification on two-dimensional turbulent flow around a square cylinder with incidence. J Eng Sci, Assiut Univ 2016;44:91–102 http://dx.doi.org/10.21608/jesaun.2016.117589
6. K.V.L. Rao, A.H. Lefebvre, Flame blowoff studies using large scale flameholders, J. Eng. Power. 104 (1982) 853, https://doi.org/10.1115/1.3227355.
7. Herbert MV. Aerodynamics influences on flame stability. Progress in Combustion Science and Technology 1980:61–109. https://doi.org/10.1016/B978-0-08-009468-7.50007-1
8. Rizk N K.Lefebvre A H. The trlationship between flame stability and drag of bluff-body flame-holders. Journal of propulsion and power, 1986, 2(4):361-365. https://doi.org/10.2514/3.22895
9. Ma Wenjie, Yang Maolin, Jin Jie, et al. Reseach on combustion performance of the aspirated edge blowing mixture cutain flame-holder. AIAA 2009-5293. https://doi.org/10.2514/6.2009-5293
10. Jeffery A L.Barry V K, Torence P B,et al. Development needs for advanced afterburner design. AIAA 2004-4192. https://doi.org/10.2514/6.2004-4192
11. Houshang B E. Overview of gas turbine augmentor design, operation and combustion oscillation. AIAA 2006-4916. https://doi.org/10.2514/6.2006-4916
12. Yang G, Jin H, Bai N. A numerical study on premixed bluff body flame of different bluff apex angle. Mathem Problems Eng 2013:1–9. 272567 http://dx.doi.org/10.1155/2013/272567
13. Boopathi S, Maran P. Effect of air pressure and gutter angle on flame, stability and DeZubay number for methane-air combustion. Int J Turbo Jet Engines 2016;34 https://doi.org/10.1515/tjj-2016-0018

14. A.M. Hamed, M.M. Kamal, A.E. Hussin "Characteristics of hollow bluff body-stabilized natural gas-air premixed flames with heat recirculation," Fuel, February 1, 2023.
15. K. Karthik, M. Vishnu, S. Vengadesan, S.K. Bhattacharyya. Optimization of bluff bodies for aerodynamic drag and sound reduction using CFD analysis. Journal of Wind Engineering & Industrial Aerodynamics 174 (2018) 133–140. https://doi.org/10.1016/j.jweia.2017.12.029
16. L Li, C Rong, S Hu, B Zhang, H Liu. Intelligent variable strut for combustion performance optimization of a wide-range scramjet engine. international journal of hydrogen energy 49 (2024). https://doi.org/10.1016/j.ijhydene.2023.05.158
17. Povinelli L. Aerodynamic drag and fuel spreading measurements in a simulated scramjet combustion module. 1974. NASAeTNeDe7674. https://ntrs.nasa.gov/citations/19740014809
18. Tao Cai, Dan Zhao, Nader Karimi. Optimizing thermal performance and exergy efficiency in hydrogen-fueled meso-combustors by applying a bluff-body. Journal of Cleaner Production 311 (2021) 127573.
19. https://doi.org/10.1016/j.jclepro.2021.127573
20. Tomas O berg. optimization of an industerial afterburner. J. Chemometrics 2003;14:5-8. http://dx.doi.org/10.1002/cem.771
21. Roham Lavimi , Alla Eddine Benchikh Le Hocine, Se´bastien Poncet, Bernard Marcos3 and Raymond Panneton. A review on aerodynamic optimization of turbomachinery using adjoint method. Institution of Mechanical Engineers, 1-37, 2024. https://doi.org/10.1177/09544062231221625
22. Ming Li, Jiaojiao Chen, Xiaoyu Feng, Feng Qu, Junqiang Bai, "An efficient adjoint method for the aero-stealth shape optimization design," Aerospace Science and Technology, November, 2023.
23. J. Brezillon , N.R. Gauger. 2D and 3D aerodynamic shape optimization using the adjoint approach. Aerospace Science and Technology 8 (2004) 715–727. https://doi.org/10.1016/j.ast.2004.07.006
24. Juanmian Lei, Jiandong He. Adjoint-Based Aerodynamic Shape Optimization for Low Reynolds Number Airfoils. Journal of Fluids Engineering, FEBRUARY 2016, Vol. 138 / 021401-1. https://doi.org/10.1115/1.4031582
25. Md Araful Hoque, Md Saifur Rahman, Khairun Nasrin Rimi, Abdur Rahman Alif, Mohammad Rejaul Haque. Enhancing formula student car performance: Nose shape optimization via adjoint method. Results in Engineering 20 (2023) 101636. https://doi.org/10.1016/j.rineng.2023.101636
26. Harry Day , Derek Ingham , Lin Ma *, Mohamed Pourkashanian. Adjoint based optimisation for efficient VAWT blade aerodynamics using CFD. Journal of Wind Engineering & Industrial Aerodynamics 208 (2021) 104431. https://doi.org/10.1016/j.jweia.2020.104431
27. Franklyn J. Kelecy., "Adjoint Shape Optimization for Aerospace Applications," Advanced Modeling & Simulation (AMS) Seminar Series NASA Ames Research Center, April 8, 2021. https://www.nas.nasa.gov/assets/nas/pdf/ams/2021/AMS_20210408_Kelecy.pdf
28. Ren, C., Zhou, H., Wu, H., Chen, Q. et al., "Aerodynamic Optimization of Vehicle Configuration Based on Adjoint Method," SAE Technical Paper 2020-01-0915, 2020, doi:10.4271/2020-01-0915. https://doi.org/10.4271/2020-01-0915
29. Comer, A. et al, Model Validation Propulsion (MVP) Workshop test case description. http://web.stanford.edu/group/ihmegroup/cgi-bin/mvpws/development.
30. Sjunnesson A., Olovsson S. and Sjöblom B., "Validation Rig – A Tool for Flame Studies", International Society for Airbreathing Engines Conference, ISABE-91-7038, Nottingham, United Kingdom, 1991. https://community.apan.org/wg/afrlcg/mvpws/p/experimental-data
31. Sjunnesson A., Nelsson C and Max E., "LDA Measurements of Velocities and Turbulence in a Bluff Body Stabilized Flame", Fourth International Conference on Laser Anemometry – Advances and Application, ASME, Cleveland, OH, 1991.
32. ghani, A., Poinsot, T., Gicquel, L., and Staffelbach, G. "LES of longitudinal and transverse self-excited combustion instabilities in a bluff-body stabilized turbulent premixed flame." Combustion and Flame, Vol. 162, 2015, pp. 4075-83. https://doi.org/10.1016/j.combustflame.2015.08.024
33. Comer, A. L ., Huang, C., Rankin, B., Harvazinski, M., and Sankaran, V. "Modeling and Simulation of Bluff Body Stabilized Turbulent Premixed Flames," 54th AIAA Aerospace Sciences Meeting, AIAA 2016-1936, San Diego, CA, 2016. https://doi.org/10.2514/6.2016-1936

34. Scott A. Drennan ,Gaurav Kumar, Rankin, and Shuaishuai Liu. “Developing Grid-Convergent LES Simulations of Augmentor Combustion with Automatic Meshing and Adaptive Mesh Refinement,” 55th AIAA Aerospace Sciences Meeting, AIAA 9-13,Grapevine , Texas, 2017. https://doi.org/10.2514/6.2017-1574
35. Menter FR. Two-equation eddy-viscosity turbulence models for engineering applications. AIAA J 1994;32:1598–605. https://doi.org/10.2514/3.12149
36. Menter FR. Zonal two-equation k-ω turbulence model for aerodynamic flows. In: AIAA paper 1993–2906; 1993. https://doi.org/10.2514/6.1993-2906